Letter

Vinyl Sulfone-Based Inhibitors of Non-Structural Protein 2 Block the Replication of Venezuelan Equine Encephalitis Virus

Huaisheng Zhang, Moeshia Harmon, Sheli Radoshitzky, Veronica Soloveva, Chris Kane, Allen J Duplantier, and Ifedayo Victor Ogungbe

ACS Med. Chem. Lett., **Just Accepted Manuscript** • DOI: 10.1021/acsmedchemlett.0c00215 • Publication Date (Web): 02 Sep 2020

Vinyl Sulfone-Based Inhibitors of Non-Structural Protein 2 Block the Replication of Venezuelan Equine Encephalitis Virus

Huaisheng Zhang,[‡] Moeshia Harmon,[‡] Sheli Radoshitzky,[ϕ] Veronica Soloveva,[ψ,†] Chris Kane,[σ] Allen J. Duplantier,[ψ] Ifedayo Victor Ogungbe[‡*]

[‡]Department of Chemistry, Physics, and Atmospheric Sciences, Jackson State University, Jackson, MS, 39217-0095

[ϕ]The Geneva Foundation, Countermeasure Development Division, U.S. Army Medical Research Institute of Infectious Diseases (USAMRIID), Frederick, MD 21702-5011

[ψ]Cherokee Nation Assurance, Countermeasure Development Division, US Army Medical Research Institute of Infectious Diseases (USAMRIID), Frederick, MD 21702-5011

[σ]Research Program Office, U.S. Army Medical Research Institute of Infectious Diseases (USAMRIID), Frederick, MD 21702-5011

ABSTRACT: Emerging infectious diseases like those caused by arboviruses such as Venezuelan equine encephalitis virus (VEEV) pose a serious threat to public health systems. Development of medical countermeasures against emerging infectious diseases are of utmost importance. In this work, an acrylate and vinyl sulfone-based chemical series was investigated as promising starting scaffolds against VEEV and as inhibitors of the cysteine protease domain of VEEV's non-structural protein 2 (nsP2). Primary screen and dose response studies were performed to evaluate the potency and cytotoxicity of the compounds. The results provide structural insights into a new class of potent non-peptidic covalent inhibitors of nsP2 cysteine protease represented by compound **11** (VEEV TrD, EC_{50} = 2.4 μM (HeLa), 1.6 μM (Vero E6). These results may facilitate the evolution of the compounds into selective and broad-spectrum anti-alphaviral drug leads.

KEYWORDS: Alphavirus, Covalent inhibitors, Cysteine protease, nsP2, Dihydroquinoline

Venezuelan equine encephalitis virus (VEEV) is a mosquito-borne neurotropic virus. VEEV infections induce flu-like symptoms, and can progress in severe cases to encephalitis and death. Fourteen antigenic subtypes of VEEV have been identified to date. Symptomatic disease in equines and humans is caused by antigenic subtypes IA/B, IC, and IE whereas subtype ID is typically avirulent in equines but virulent in humans.[1,2] New World alphaviruses like VEEV, eastern equine encephalitis virus (EEEV), and western equine encephalitis virus (WEEV) are widely distributed in North, Central and South America. Occasional outbreaks of VEEV have been reported over the years in the Americas.[3,4] The use of VEEV as a bioweapon was evaluated by both the US and Russia during the Cold War.[5] New World alphaviral infections used to be very rare in the US (<10 cases per year) which made the feasibility of clinical trials for anti-alphaviral therapeutics challenging. But in 2019, a record high number of EEEV cases was reported in the US with at least 14 fatalities.[6] Also, acute infections caused by the related Old-World alphavirus, Chikungunya virus (CHIKV), are becoming more common, and to date, over 1 million cases have been reported worldwide. Old-World alphaviruses present significant risk to healthcare systems and livelihood of millions of people in the tropics and subtropical regions.[7-9]

VEEV has a single-stranded, positive-sense RNA genome that is ~11.4 kb in size. One of the two open reading frames in the alphavirus genome encodes the non-structural polyprotein precursor nsP1234. Its final products, viral non-structural proteins (nsP1, nsP2, nsP3 and nsP4), are obtained via proteolytic hydrolysis of the polyprotein precursor by virus-encoded cysteine protease (nsP2). Replication of the viral genome as well as the transcription of its 26S subgenomic viral RNA relies on the biochemical actions of nsP1-4. The viral structural proteins, capsid protein (CP), small peptides (E3 and 6K), and the envelope glycoproteins (E1 and E2) are translated from the 26S subgenomic viral RNA. VEEV nsP2 is an important drug target due to the crucial roles it plays in the virus lifecycle. Apart from proteolytic hydrolysis of the non-structural polypeptide precursor into functional protein units, nsP2 regulates negative strand RNA synthesis via its methyltransferase activity. In addition, nsP2 facilitates the packaging of genomic RNA into virus particles.[10]

To date, only a few compounds including CA-074Me and E64-d have been reported to inhibit both the protease activity of VEEV's nsP2 and the replication of VEEV, albeit marginally.[11,12] It is important to point out, however, that a series of benzamidine-based and potent inhibitors of VEEV that inhibit viral RNA synthesis is currently under pre-clinical investigation.[13,14] In this work, a phenotypic screening-based approach was used to identify compounds with antiviral activity against VEEV from a library of potential covalent protease inhibitors.[15,16] An initial structure-activity relationship (SAR) studies was used to define the pharmacophore in the hit compound (**1**) as well as the in-

hibitory activity of its analogues against the nsP2 protease (**10, 11**). Interactions between the protease and the active compounds (**10-13**) were investigated via covalent molecular docking.

We used a library derived from our previously reported fragment-based approach to identify protease inhibitors of VEEV IC-SH3.[15] VEEV IC-SH3 is a virulent strain derived from a human isolate from a VEE outbreak in 1992–1993 in Venezuela.[17] Our initial screening efforts against VEEV (IC-SH3)-infected Vero and HeLa cells identified an acrylate-based 1,2-dihydroquinoline derivative, **1**, as a potent VEEV inhibitor (EC_{50}'s of 0.55 μM (Vero) and 6.48 μM (HeLa)). Subsequent studies to develop SAR around compound **1** were initiated to i) understand which structural motifs are necessary for inhibition of VEEV's replication, ii) determine if the *α*, *β*-unsaturation in the acrylate warhead is crucial for inhibition (compounds **2-8**), iii) determine if similar warheads like methyl vinyl sulfone and phenyl vinyl sulfone are tolerated, iv) determine the tolerability of substituents at the γ-carbon, and v) determine if the dihydroquinoline heterocycle can be replaced by similar bicyclic motifs. Analogues were synthesized as outlined in **Scheme 1**. The structures, detailed description of synthesis and characterization of all analogs (**2-43**) investigated are described in the supporting information. The compounds were prepared from either 3-amino-1,2-propanediol or 2-amino-1-propanol by Boc-protection followed sequentially by either periodate oxidation (**1-4** and **9-11**) or Dess–Martin periodinane oxidation (**12-16**), then Horner-Wadsworth-Emmons olefination of the resulting aldehyde with appropriate phosphonate, removal of the Boc group by treatment with TFA, and final amide coupling with the appropriate acid in the presence of HBTU. Compounds **5-8** were readily available by analogous amide coupling starting with methyl 4-aminobutyrate.

This initial SAR study revealed that i) partial saturation of the dihydroquinoline ring is tolerated (**2**), ii) methyl substituents at the 2- and/or 4-position of the hydroquinoline motif improve anti-VEEV activity (**1** and **2** vs **4**), iii) methyl substitution at carbon 6 of the 1,2-dihydroquinoline ring decreases antiviral activity, and iv) the *α*, *β*-unsaturation of the acrylate warhead is required for anti-VEEV activity (**Table 1**). Subsequent analogs were evaluated against VEEV-TC83 using neuronal cell lines including human BE(2)-M17 and mouse Neuro-2a cells which may be more physiologically relevant *in vitro* models as they better represent primary targets of VEEV infection. VEEV-TC-83 is a live-attenuated virus generated by serial passage of VEEV Trinidad (TrD) strain in guinea pig heart cells. Work with this virus can be performed in BSL-2 and therefore for most assays hereon this variant was used.[18]

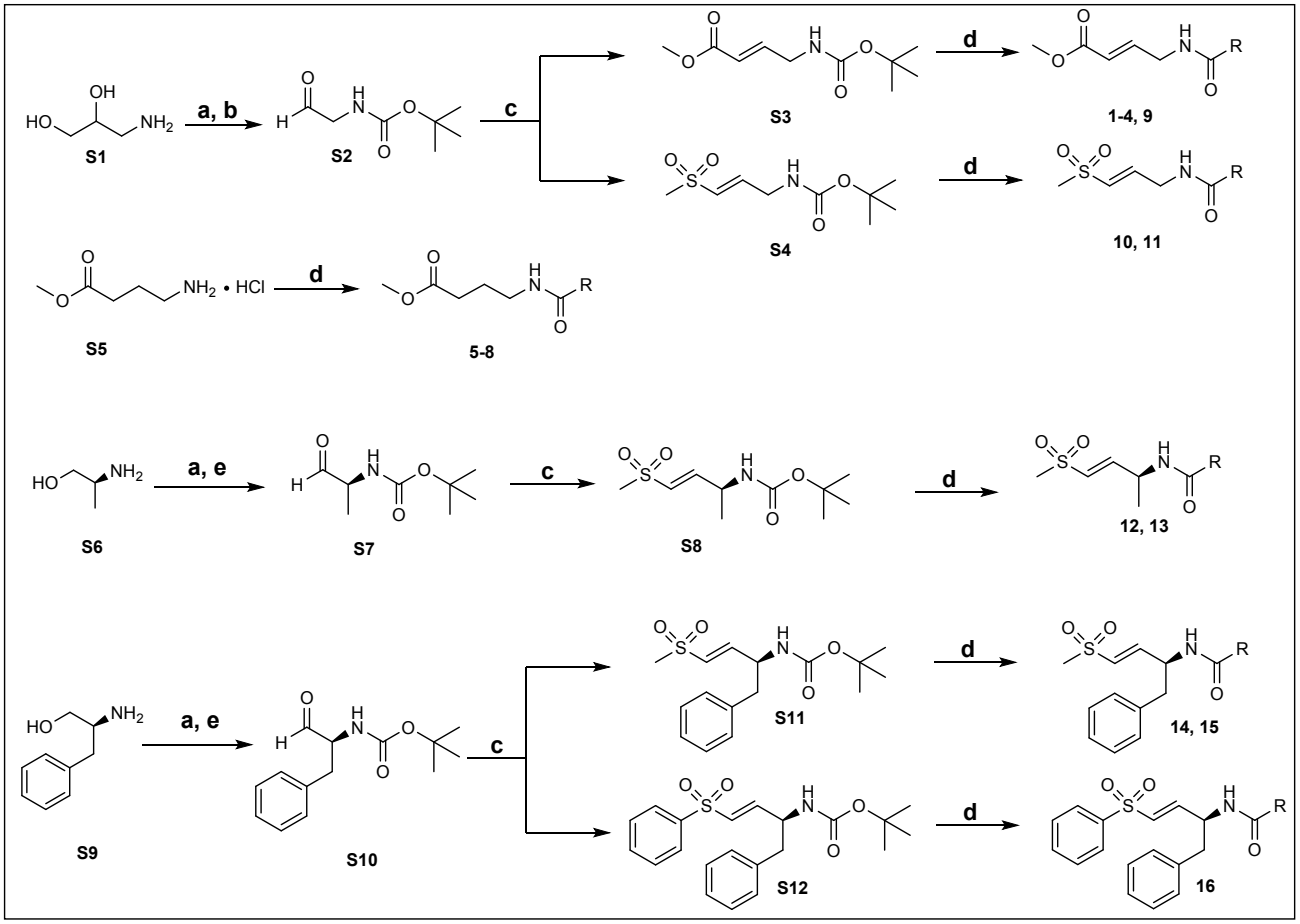

Scheme 1. Synthesis of target compounds **1-16**. Reagents and conditions: (**a**) CH_2Cl_2:CH_3OH, Et_3N, Boc_2O, 23°C, 2 h, >90%; (**b**) H_2O, $NaIO_4$, RT, 1 h, 64%; (**c**) NaH, THF, methyl diethylphosphonoacetate, diethyl((methylsulfonyl)methyl) phosphonate or diethyl((phenylsulfonyl)methyl) phosphonate, 0°C, 25 min, 40-70%; (**d**) 33% TFA in DCM, 0°C, 1.5 h. Then ACN, R-COOH, Et_3N, HBTU, RT, 16 h, 30-40%; (**e**) DMP, H_2O-DCM, 23°C, 1 h, 40-60%.

Table 1. Anti-VEEV activity of compounds 1-8.

Compound		1-4 / 5-8					
		HeLa (VEEV IC-SH3)			VeroE6 (VEEV IC-SH3)		
	R	EC_{50} (μM)	CC_{50} (μM)	SI	EC_{50} (μM)	CC_{50} (μM)	SI
1	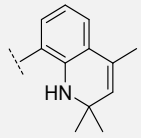	0.6 ± 0.1	>30	>55	6.5 ± 2.0	>30	>5
2	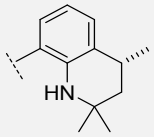	1.2 ± 0.1	>30	>26	8.2 ± 3.1	>30	>4
3	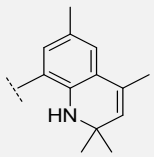	8.7 ± 0.8	>30	>4	8.6± 2.5	>30	>3.5
4	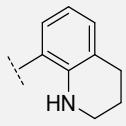	18 ± 1	>30	>2	>30	>30	-
5	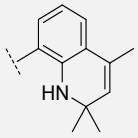	>30	>30	-	>30	>30	-
6	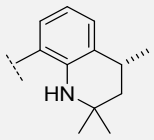	>30	>30	-	>30	>30	-
7	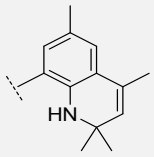	>30	>30	-	>30	>30	-
8	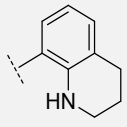	>30	>30	-	>30	>30	-
RIID reference control E		0.21 ± 0.02	>3	>12	0.14 ± 0.03	>3	>18

The compounds were tested at concentrations of 13.72 nM-30 μM (8 doses, 3-fold dilution). HeLa and VeroE6 cells were treated with the indicated compounds and 2 h later inoculated with VEEV IC-SH3 (MOI=0.1 and 0.01, respectively). After 20 h, cells were fixed, and stained with antibodies against E2. High-content quantitative image-based analysis was used to measure relative infection rates.

Substitution of the acrylate warhead with methyl sulfone (e.g., **10-13, 15**) provided low micromolar potency in both neuronal cell lines (**Table 2**). This result was particularly encouraging since the methyl sulfone, as opposed to an ester, is not prone to metabolic hydrolysis. It is also interesting that while substitution at the γ-carbon of methyl esters was not tolerated, mono-substitution of either a methyl or benzyl group on the γ-carbon of sulfone derivatives retained anti-VEEV activity.

Table 2. Anti-VEEV activity of selected analogues. See Table S1 for full list of analogues.

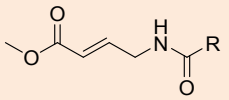

1, 2, 9

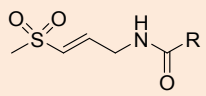

10, 11

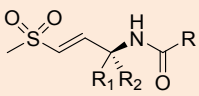

12-13: R_1 = CH_3 and R_2 = H

14-15: R_1 = Benzyl and R_2 = H

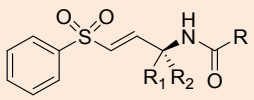

16: R_1 = Benzyl and R_2 = H

Compound	R	Human BE(2)-M17			Mouse Neuro-2a			Virus
		EC_{50} (μM)	CC_{50} (μM)	SI	EC_{50} (μM)	CC_{50} (μM)	SI	
1	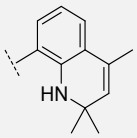	4.5 ± 3.5	6.7	1.5	>25	18.1	-	TC83
2	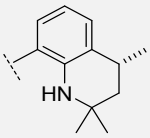	>25	11	-	22 ± 11	>25	>1	TC83
9	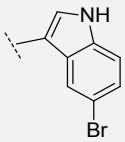	3 ± 5	12	4	11 ± 5	>25	>2	TC83
10	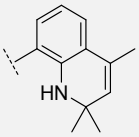	2.0 ± 1.3	19.6	>9	5 ± 2	27	>5	TC83
		5 ± 1[a]	30[a]	7[a]	1.4 ± 0.1[b]	>30[b]	>22[b]	TrD
		6 ± 1[c]	>25[c]	> 4[c]	-	-	-	TC83
11	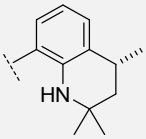	1.4 ± 1.0	>25	>18	2 ± 1	>25	>12	TC83
		2.4 ± 0.5[a]	30[a]	>12[a]	1.6 ± 0.1[b]	>30	>19[b]	TrD
		8 ± 1[c]	48[c]	6[c]	-	-	-	TC83
12	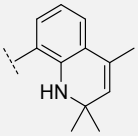	4.5 ± 0.2	>25	>5	3.4 ± 0.1	>25	>7.3	TC83
		2.7 ± 0.2[c]	>25[c]	> 9.7[c]	-	-	-	TC83
13	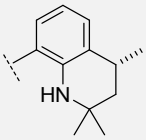	3.3 ± 0.2	>25	>7.5	3.7 ± 0.2	>25	>7	TC83
14	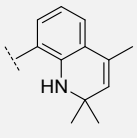	17 ± 3	>38	>2	13 ± 6	>50	>4	TC83
15	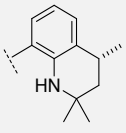	9.3 ± 2.8	>50	>5.4	13 ± 9	>50	>4	TC83

Compounds 1, 2, 9-13 were tested at concentrations of 11.43 nM-25 μM (8 doses, 3-fold dilution) whereas compounds 14-16 were tested from 22.86 nM-50 μM (8 doses, 3-fold dilution). BE(2)-M17 and Neuro-2a cells were treated with the indicated compounds and 2 h later inoculated with VEEV TC83 (MOI = 1.2 and 3.5, respectively). After 7 h, cells were fixed, and stained with antibodies against E2. High-content quantitative image-based analysis was used to measure relative infection rates. [a] Compounds were assayed in VEEV Trinidad-infected Vero cells (MOI = 0.01). [b] Compounds were assayed in VEEV Trinidad-infected HeLa cells (MOI = 0.1).). [c] Compounds were assayed in VEEV TC83-infected mouse cortical neurons (MOI = 0.04) Cells were fixed 20 h after virus inoculation and stained and analyzed as above.

Table 2 Continued. Anti-VEEV activity of selected analogues. See Table S1 for full list of analogues.

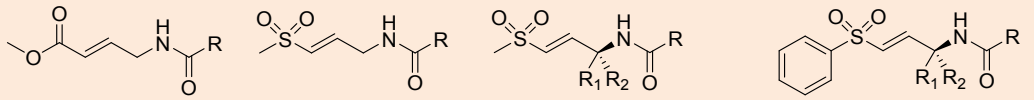

Compound	R	Human BE(2)-M17			Mouse Neuro-2a			Virus
		EC_{50} (μM)	CC_{50} (μM)	SI	EC_{50} (μM)	CC_{50} (μM)	SI	
16	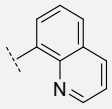	17 ± 5	16	1	19 ± 15	46	>2	TC83
ML336	Ref. 13	0.01 ± 0.00	>2.5	>250	0.02 ± 0.01	>2.5	>125	TC83

Compounds 1, 2, 9-13 were tested at concentrations of 11.43 nM-25 μM (8 doses, 3-fold dilution) whereas compounds 14-16 were tested from 22.86 nM-50 μM (8 doses, 3-fold dilution). BE(2)-M17 and Neuro-2a cells were treated with the indicated compounds and 2 h later inoculated with VEEV TC83 (MOI = 1.2 and 3.5, respectively). After 7 h, cells were fixed, and stained with antibodies against E2. High-content quantitative image-based analysis was used to measure relative infection rates.

Compounds **10**-**12** were also evaluated against VEEV-TC83 using mouse primary cortical neurons, and the compounds displayed anti-VEEV activity (**Table 2**). Finally, we conclude that the di- and tetra-hydroquinoline of sulfone derivatives retained anti-VEEV activity since replacement with the fully unsaturated quinoline (**16**) did not result in anti-VEEV activity. Additional replacements of the unsaturated quinoline ring that led to inactivity are listed in Table S1 (supporting information). It is worth pointing out that different MOIs and infection times were used for the assays in the different cell lines (to achieve 50-80% infection rates at the study endpoint). These variations might have contributed to the observed EC_{50} difference. Also, infection kinetics (such as the length of one virus lifecycle) might be different between the cells used. Finally, these differences might be also due to non-specific effects of the compounds on the cells. Overall, compounds **10-13** were the most active analogues in neuronal cells in this initial SAR study.

To confirm the mechanism of action for this series of VEEV inhibitors, representative compounds were tested for their ability to inhibit the proteolytic activity of nsP2 in vitro. The protease was recombinantly expressed, purified, and assayed using the gel discontinuous assay previously reported by Legler and co-workers.[12] As shown in **Figure 1** and **S1**, compounds **11-13** inhibited the proteolytic activity of VEEV nsP2 in a dose-dependent manner. At 20 μM, compounds **11-13** completely inactivated VEEV nsP2 (1 μM) in the presence of V12 substrate (a CFP-YFP FRET Substrate, 10 μM; data not shown). At 0.9 μM, the estimated percentage inhibition after 24 h incubation was 39%, 59% and 71% for **11, 12** and **13**, respectively. Covalent molecular docking was used to predict favored binding orientations and specific binding interactions of the compounds with the nsP2 protein. As shown in **Figure 2** and **3**, compound **11**, which was the most selective in VEEV-infected BE(2)-M17 and Neuro-2a cells, was predicted to have significant Van der Waals interactions with Try 547, Asn 545, Ala 509 and His 510, and complex-stabilizing hydrogen bonding interactions with Asn 545, His 510 and a key water molecule within the active site.

The methyl sulfone motif as well as methyl substituents of the tetrahydroquinoline ring are predicted to be partially exposed to solvent, and thus these moieties may provide an avenue for physicochemical property modifications to reduce microsomal clearance. Co-crystallization of nsP2 with selected inhibitors, in order to determine the preferred binding modes of the compounds, is under active investigation.

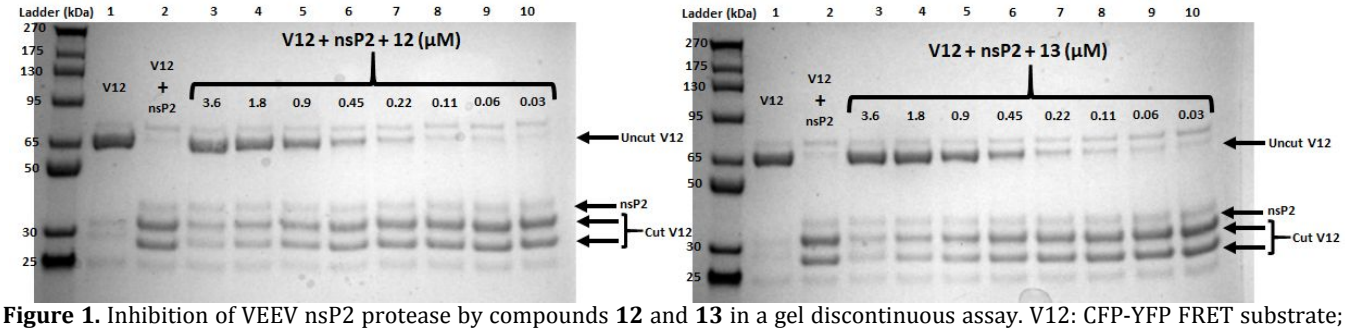

Figure 1. Inhibition of VEEV nsP2 protease by compounds **12** and **13** in a gel discontinuous assay. V12: CFP-YFP FRET substrate; nsP2: tag-free non-structural protease 2. For both gels, Lane 1 is V12 alone, Lane 2 is V12 + nsP2, Lanes 3-10 are V12 + nsP2 + **12** or **13** at 3.6, 1.8, 0.9, 0.45, 0.22, 0.11, 0.06 and 0.03 μM, respectively. The molecular weight (MW) of uncut V12, the two V12 fragments (cut v12) and tag-free nsP2 are 58.3, 30.9, 27.4, and 38.29 kDa, respectively. The reactions were carried out in 50 mM HEPES buffer pH 7.4 for 24 h at room temperature. The concentrations of VEEV nsP2 and V12 were 1 μM and 10 μM, respectively.

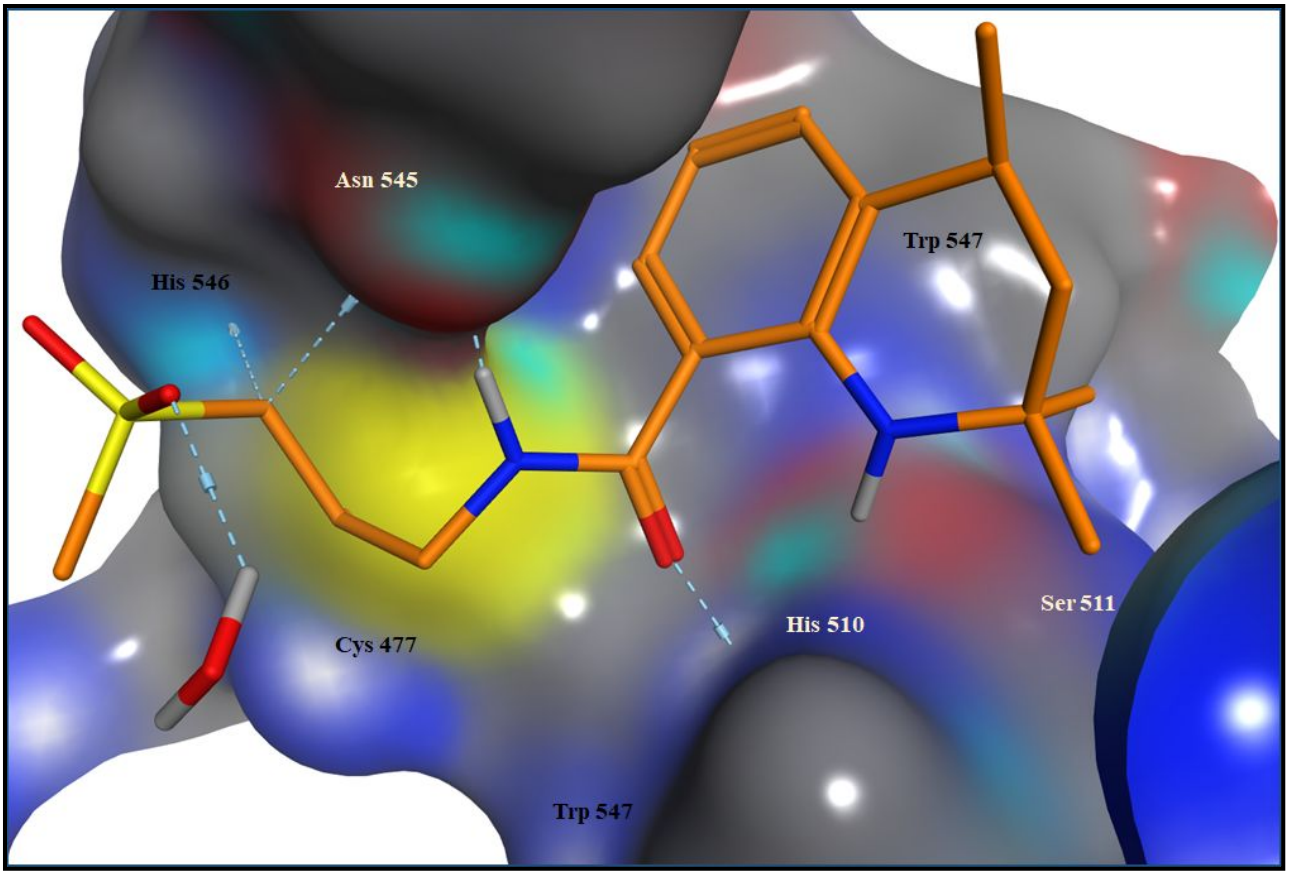

Figure 2. Modelled complex of VEEV nsP2 and compound **11**. The highlighted residues are predicted to have significant Van der Waals interactions (piecewise linear potential) with compound **11**. The blue dash depicts H-bond interaction. The figure was prepared using Molecular Operating Environment (MOE).

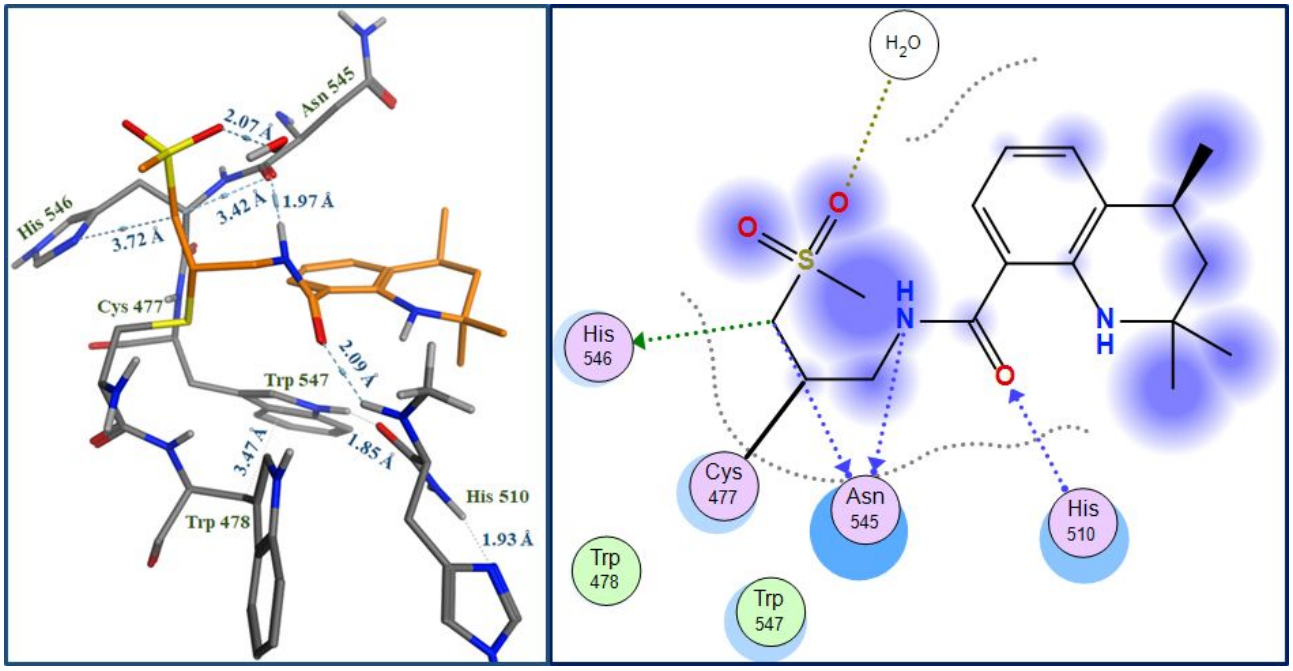

Figure 3. Modelled complex of VEEV nsP2 and compound **11**. The left panel is a stick model representation of the predicted network of H-bond interactions (depicted as the blue dash lines) stabilizing the nsP2-**11** complex. Asn 545, His 510 and His 546 residues are predicted to have direct H-bond interactions with compound **11**. Carbon atoms are depicted as yellow in **11**. The right panel is a 2D depiction of the proximity (gray contour) of active site residues to compound **11** as well as the extent of exposure (purple hue) of the compound's atoms to solvent. The figure was prepared using Molecular Operating Environment (MOE).

In summary, a new series of non-peptidic dihydroquinoline and tetrahydroquinoline-based covalent inactivators of VEEV's nsP2 cysteine protease was identified in this work. The preliminary SAR study showed that the conformationally more flexible dihydroquinoline and tetrahydroquinoline rings provides an appropriate shape for effective binding at the active site. Ongoing and future work will focus on improving microsomal stability and potency, determination of *in vivo* pharmacokinetics and tolerability, and subsequent evaluation in an animal model of VEEV infection

ASSOCIATED CONTENT

Supporting Information

The Supporting Information is available free of charge on the ACS Publications website. Supplementary data and details of assays, synthesis and compound characterization are provided as supporting information (PDF).

AUTHOR INFORMATION

Corresponding Author

*ifedayo.v.ogungbe@jsums.edu; +1 601-979-3719

Present Addresses

† Merck Research Laboratories, Cambridge, MA, USA.

Author Contributions

The manuscript was written through contributions of all authors.

Funding Sources

This work was carried out in part by resources made available by the US National Institutes of Health (SC3GM122629 and G12MD007581). MH was supported by NIH-RISE (5R25GM067122) and was a participant in the Naval Research Laboratory (NRL) HBCU/MI Summer Internship Program sponsored by the Office of Naval Research (N0017315RMV04). Cell-based VEEV screening at USAMRIID was funded by The Joint Science and Technology Office for Chemical and Biological Defense (JSTO-CBD) of the Defense Threat Reduction Agency (DTRA) under plan number CB10217. The funding agency had no involvement in any aspect of the study including design, data collection, analysis, interpretation, or composition of this manuscript. The opinions, interpretations, conclusions, and recommendations expressed here are those of the authors and do not represent those of the U.S. Army, U. S. Department of Defense or the U. S. government.

ACKNOWLEDGMENT

We thank Dr. Pat. Legler (NRL, Washington DC) for very helpful discussions about nsP2, and for providing the nsP2 and V12 plasmids.

ABBREVIATIONS

DCM, dichloromethane; ACN, acetonitrile; DMP, Dess–Martin periodinane; HBTU, *N*,*N*,*N*′,*N*′-Tetramethyl-*O*-(1*H*-benzotriazol-1-yl)uronium hexafluorophosphate.

REFERENCES

(1) Aguilar, P.V.; Estrada-Franco, J.G.; Navarro-Lopez, R.; Ferro, C.; Haddow, A.D.; Weaver, S.C. Endemic Venezuelan equine encephalitis in the Americas: hidden under the dengue umbrella. *Future Virol.* **2011**, *6*, 721-740.

(2) Sharma, A; Knollmann-Ritschel, B. Current understanding of the molecular basis of Venezuelan equine encephalitis virus pathogenesis and vaccine development. *Viruses* **2019**, *11*, 164.

(3) Carrera, J.P; Bagamian, K.H.; Travassos da Rosa, A.P.; Wang, E.; Beltran, D.; Gundaker, N.D.; Armien, B.; Arroyo, G.; Sosa, N.; Pascale, J.M.; Valderrama, A.; Tesh, R.B.; Vittor, A.Y.; Weaver, S.C. Human and equine infection with alphaviruses and flaviviruses in Panamá during 2010: a cross-sectional study of household contacts during an encephalitis outbreak. *Am. J. Trop. Med. Hyg.* **2018**, *98*, 1798-1804.

(4) Zacks, M.A.; Paessler, S. Encephalitic alphaviruses. *Vet. Microbiol*. **2011**, 140, 281-286.

(5) Reichert, E.; Clase, A.; Bacetty, A.; Larsen, J. Alphavirus antiviral drug development: scientific gap analysis and prospective research areas. *Biosecur. Bioterror.* **2009**, *7*, 413-427.

(6) Morens, D.M.; Folkers, G.K.; Fauci, A. S. Eastern equine encephalitis virus — another emergent arbovirus in the United States. *N. Engl. J. Med.* **2019**, *381*, 1989-1992.

(7) Kosasih H.; de Mast, Q.; Widjaja, S.; Sudjana, P.; Antonjaya, U.; Ma'roef, C.; Riswari, S.F.; Porter, K.R.; Burgess, T.H.; Alisjahbana, B., van der Ven, A. Evidence for Endemic Chikungunya Virus Infections in Bandung, Indonesia. *PLoS Negl. Trop. Dis*. **2013**, *7*, e2483.

(8) Lemant, J.; Boisson, V.; Winer, A.; Thibault, L.; André, H.; Tixier, F.; Lemercier, M.; Antok, E.; Cresta, M.P.; Grivard, P.; Besnard, M.; Rollot, O.; Favier, F.; Huerre, M.; Campinos. J.L.; Michault, A. Serious acute chikungunya virus infection requiring intensive care during the reunion island outbreak in 2005–2006. *Crit. Care Med*. **2008**, *36*, 2536–2541.

(9) Angelini, P.; Macini, P.; Finarelli, A.C.; Pol, C.; Venturelli, C.; Bellini, R.; Dottori, M. Chikungunya epidemic outbreak in Emilia-Romagna (Italy) during summer 2007. *Parasitologia* **2008**, *50*, 97–98.

(10) Kim, D. Y.; Atasheva, S.; Frolova, E. I.; Frolov, I. Venezuelan equine encephalitis virus nsP2 protein regulates packaging of the viral genome into infectious virions. *J. Virol*. **2013**, *87*, 4202–4213.

(11) Campos-Gomez, J.; Ahmad, F.; Rodriguez, E.; Saeed, M.F. A novel cell-based assay to measure activity of Venezuelan equine encephalitis virus nsP2 protease. *Virology* **2016**, *496*, 77-89.

(12) Hu, X.; Compton, J.R.; Leary, D.H.; Olson, M.A.; Lee, M.S.; Cheung, J.; Ye, W.; Ferrer, M.; Southall, N.; Jadhav, A.; Morazzani, E.M. Glass, P.J; Marugan, J. and Legler, P.M. Kinetic, mutational, and structural studies of the Venezuelan equine encephalitis virus nonstructural protein 2 cysteine protease. *Biochemistry* **2016**, *55*, 3007-3019.

(13) Skidmore, A.M.; Adcock, R.S.; Jonsson, C.B.; Golden, J.E.; Chung, D.H. Benzamidine ML336 inhibits plus and minus strand RNA synthesis of Venezuelan equine encephalitis virus without affecting host RNA production. *Antiviral Res.* **2020**, *174*, 104674.

(14) Jonsson, C.B.; Cao, X.; Lee, J.; Gabbard, J.D.; Chu, Y.K.; Fitzpatrick, E.A.; Julander, J.; Chung, D.H.; Stabenow, J.; Golden, J.E. Efficacy of a ML336 derivative against Venezuelan and eastern equine encephalitis viruses. *Antiviral Res.* **2019**, *167*, 25-34.

(15) McShan, D.; Kathman, S.; Lowe, B.; Xu, Z.; Zhan, J.; Statsyuk, A.; Ogungbe, I.V. Identification of non-peptidic cysteine reactive fragments as inhibitors of cysteine protease rhodesain. *Bioorg. Med. Chem. Lett.* **2015**, *25*, 4509-4512.

(16) Kathman, S.G.; Xu, Z.; Statsyuk, A.V. A fragment-based method to discover irreversible covalent inhibitors of cysteine proteases. *J. Med. Chem.* **2014**, *57*, 4969-4974.

(17) Rico-Hesse, R.; Weaver, S.C.; De Siger, J.; Medina, G.; Salas, R.A. Emergence of a new epidemic/epizootic Venezuelan equine encephalitis virus in South America. *Proc. Natl. Acad. Sci. U.S.A.* **1995**, *92*, 5278-5281.

(18) Berge, T.O.; Banks, I.S.; Tigertt, W.D. Attenuation of Venezuelan equine encephalomyelitis virus by ire vitro cultivation in guinea-pig heart cells. *Am. J. Hyg.* **1961**, *73*, 209-218.

TOC Graphic

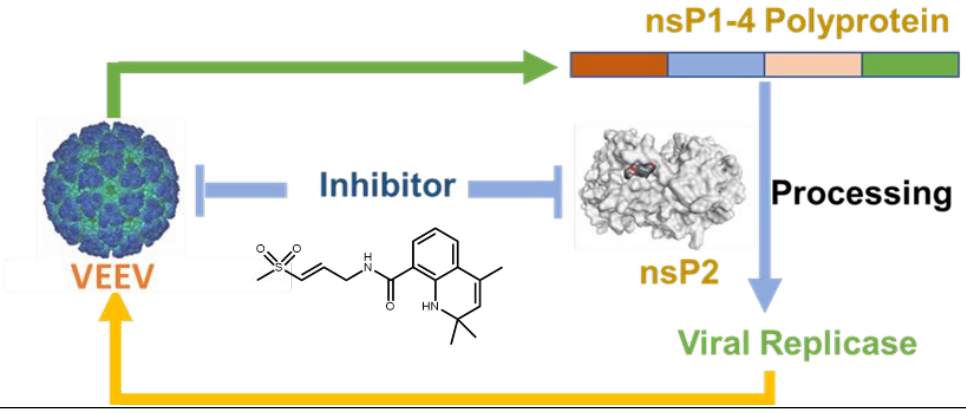
nsP1-4 Polyprotein
Inhibitor
Processing
VEEV
nsP2
Viral Replicase